Thermodynamic Simulation 2022

by Anton Irawan

ORIGINAL PAPER

Thermodynamics Simulation Performance of Rice Husk Combustion with a Realistic Decomposition Approach on the Devolatilization Stage

Soen Steven[1] · Pandit Hernowo[2] · Elvi Restiawaty[1,3] · Anton Irawan[4] · Carolus Borromeus Rasrendra[1,5] · Abrar Riza[6] · Yazid Bindar[1,7]

Abstract

The high calorific value of rice husk and rich silica content in rice husk ash make its valorization becomes attractive. This study presents the thermodynamics simulation performance of rice husk combustion using a realistic decomposition approach. A non-ideal gas approach and fugacity coefficient were also considered in the calculation. In this study, devolatilization of rice husk is simulated to form gas (64.78%), liquid/tar (7.28%), solid/char (27.94%), and all of these are then oxidized with 100% excess air to form flue gas. From the calculation, about 2.6 MJ/kg of specific combustion energy is produced. The maximum combustion temperature in the furnace is up to 1457 °C for perfect insulation and up to 1400 °C if there is a 5% heat loss due to radiation. Furthermore, the thermodynamics simulation expressed that NO_X emission amount from rice husk combustion is negligible and there is still a probability for CO and H_2 to be produced at above 500 °C due to Boudouard reaction and homogeneous water gas shift reaction (WGSR). It is found that combustion equipped with larger excess air could quench the heat produced and reduce the combustion efficiency but could maintain the temperature at 700 °C. Supplying excess air of about 180–200% is advantageous to keep the combustion temperature at 700 °C to avoid silica crystalline formation which harms human health, as well as suppressing NO_X emission and reducing CO emission from the simultaneous reaction of Boudouard-WGSR. Finally, the study concluded that a realistic decomposition approach could predict the rice husk combustion performance with reasonable and logical results.

Graphical Abstract
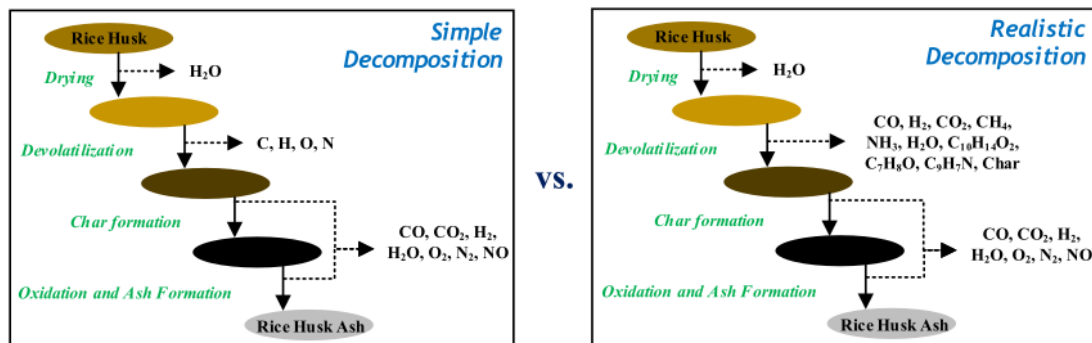
Keywords Biomass · Degree of freedom · Flue gas · Adiabatic flame temperature · Air to fuel ratio

✉ Yazid Bindar
ybybyb@fti.itb.ac.id

Extended author information available on the last page of the article

Statement of Novelty

So far, many established studies have proposed a simple approach to the devolatilization stage. This is unrealistic because biomass decomposition is assumed to form C, H, O, N elements before entering oxidation. In the realistic decomposition approach, biomass decomposition is not to form C, H, O, N elements but gas, liquid/tar, and carbon as solid/char. Interestingly, there is still a lack of study on it and therefore, this study discussed the rice husk combustion simulation performance with a realistic decomposition approach on the devolatilization stage. The results perform that this approach gives a reasonable agreement with the other researchers' results in terms of the amount and composition of devolatilized product, the amount of specific combustion energy, adiabatic flame temperature, and flue gas composition.

Introduction

Recently, biomass utilization for alternative fossil fuel and chemicals surrogates has become a major concern due to its positive impact on humans and the environment [1, 2]. One of the abundantly available biomass in Indonesia is rice husk [3]. They have several superior properties, i.e. mostly occupies approximately 20 wt% from straw-free rice plant [4], have a calorific value in the range of 12–17 MJ/kg [5], have an ash content in rice husk of nearly 20 wt% [6–8], and contain silica in ash as much as 80–98 wt% [9, 10]. The high calorific value, as well as the rich silica content in ash, make them important and interesting to be valorized. The valorization can be implemented through rice husk combustion in a furnace to produce energy and ash then followed by rice husk ash extraction to acquire silica [4, 9–11]. There are several stages occurred in the rice husk combustion, namely drying, devolatilization, char formation, further oxidation, and ash formation [5, 6, 12, 13].

Over the past few decades, studies on thermodynamics simulation have been able to predict combustion performance which mainly focused on specific combustion energy calculation, rice husk combustion temperature monitoring, as well as flue gas composition prediction and analysis. A study on combined heat power fuelled by rice husk with electricity output up to 1.15 MW gave a specific rice husk consumption of 1.2–1.7 kg/kWh [14] or recalculated as specific energy produced in the range of 2.12–3.00 MJ/kg. Apart from that, the case study from Pakistan stated that as much as 4947.28 MWh of energy could be generated from the combustion of 6432 tonnes of rice husk [15] or equal to specific combustion energy of about 2.77 MJ/kg. Besides, the energy balance evaluation on 2.8 g/s rice husk combustion

for steam and hot air generation resulted in 21.09 kJ/s of utilized energy [16] and it is equal to approximately 7.53 MJ/kg of specific energy released. Meanwhile, the rice husk combustion modelling study in a grate bed furnace showed a maximum combustion temperature of 1407 °C and flue gas exhaust temperature of 694 °C with the composition of N_2, CO, CO_2, H_2O, and remaining O_2 [17].

In addition, the detailed investigation of biomass combustion performance in a more complex furnace type was mostly done with the aid of computational fluid dynamics (CFD) study. Biomass combustion in a simple grate furnace is widely applied for domestic application but the harmful emission is imperative to be minimized by numerical optimization [18]. The packed bed furnace is also utilized to upgrade the combustion performance but is also believed to be challenging both in experimentation and in data collection [2, 19]. Due to the high problem complexity, normal CFD codes are not even able to model the solid (biomass) behavior and transformation in the furnace [2]. Hence, the inclusion of user-defined functions or sub-routines for modelling biomass drying, biomass devolatilization, char oxidation, solid–gas contact, should be embedded manually [18–20].

The adversity of biomass combustion CFD modelling can be overcome by replacing the biomass input stream with its decomposed products [21, 22]. The ability to calculate the biomass decomposition products at a certain temperature, thus, becomes important. Unfortunately, many studies and well-established textbooks proposed that at the devolatilization stage, biomass decomposes to C, H, O, N elements prior to being oxidized [23–25]. This approach is simple but imprecise so it should be corrected with another approach. The proposed approach is realistic decomposition, where rice husk devolatilization products are not C, H, O, N elements but gas, liquid/tar, and solid/char [23]. To avoid misinterpretation, the term "realistic" is not about emphasizing the realistic product composition compared to the experiment results, but in terms of its realistic decomposition behavior.

The study by Thunman et al. has succeeded to build the model using mass and energy balances for predicting actual volatile gas composition from wood devolatilization [26]. However, the discussion still lay on the volatile gas composition and no further examination about the thermodynamics aspects of biomass combustion. Therefore, this study intends to discuss the thermodynamics simulation performance of rice husk combustion with a realistic decomposition approach. The discussion comprises of problem preliminary analysis, devolatilized products prediction, specific energy calculation from rice husk combustion, adiabatic flame temperature determination, air supply strategy for maintaining rice husk combustion temperature, and the flue gas

composition analysis due to the attendance of Boudouard reaction and homogeneous water gas shift reaction (WGSR).

Methods

Degree of Freedom (DoF) Calculation Procedure

The DoF calculation aims to state the number of unknown variables and equations involved to solve the mass and energy balances problem until a unique solution is acquired. It was done for mass balance and mass-energy balance. To simplify the problem, it is recommended to create a simple block diagram complete with flowrate symbol and component symbol. Afterward, the known and unknown variables should be identified before DoF calculation was executed [25]. The DoF calculation follows Eq. 1a for mass balance and Eq. 1b for mass-energy balance.

$$DoF\,(mass\,balance) = SV_M - LIE - KD_M - SE \tag{1a}$$

$$DoF(mass - energy\,balance) = SV_M + SV_E - LIE - EE - KD_M - KD_E - SE \tag{1b}$$

where SV_M is the total number of mass stream variables, LIE is the number of linearly independent equations, KD_M is the number of known data for mass stream, SE is the number of supplementary equations, SV_E is the number of energy stream variables, EE is the number of energy equation (always 1), and KD_M is the number of known data for energy stream.

The number of stream variables consists of the total of inlet and outlet streams (include energy stream variables for mass-energy balance DoF calculation). The linearly independent equations are the total elements involved in the problem (include energy equation for mass-energy balance DoF calculation). The stream which contains pure concentration (100%) no need to be involved in DoF calculation. If there is a calculation basis or known flowrate, they have to be involved in the DoF calculation as known data (also include known energy variables for mass-energy balance DoF calculation). Additionally, supplementary equations are equations besides mass and energy balance equations.

Realistic Decomposition Calculation

The rice husk used in this study has a calorific value of 14.95 MJ/kg whereas the properties comprised of ultimate and proximate analysis in dry basis condition are given in Table 1. The proximate analysis is performed at 900 °C for 7 min following ASTM 3175-07 procedure [24], whereas the actual decomposition in this study occurred at $T=700$ °C. This will lead to the distiction between the volatile matter

Table 1 Ultimate and proximate analysis of rice husk (dry basis)

Ultimate analysis		Proximate analysis	
C	37.95 wt%	Moisture	–
H	5.41 wt%	Volatile matter	63.86 wt%
O	36.56 wt%	Fixed carbon	17.02 wt%
N	0.96 wt%	Ash	19.12 wt%

measured from proximate analysis (Y_{VM}) and the actual volatile produced (Y_{VY}). The ratio between Y_{VY} and Y_{VM} is defined as volatile enhancement factor (V_E) which plays a role to correct the amount of devolatilized products at a temperature other than 900 °C. The value is commonly in the range of 0.8–1.3 [23].

In order to determine V_E, the biomass type number (N_{CT}) should be calculated first as in Eq. 2a. The N_{CT} value was then applied to determine the predicted volatile matter mass fraction (Y'_{VM}), Eq. 2b. Subsequently, Eq. 2c is a temperature correction function, $f_5(T)$ in °C unit, which was later employed in Eq. 2d to obtain the predicted devolatilized products mass fraction (Y'_{VY}). Afterward, V_E was calculated following Eq. 2e [23, 24]. The devolatilized products consist of gas, liquid, and solid. Gas was represented with CO, H_2, CO_2, CH_4, H_2O, and NH_3 [27, 28], liquid or tar is assumed to consist of $C_{10}H_{14}O_2$ (2-methoxy-5-propyl-phenol), C_7H_8O (cresol), and C_9H_7N (quinoline) [29], and solid/char was presumed to contain only carbon [28]. Each product amount was determined from Eqs. 3a-3e and should be consistent with the value from dry-ash-free basis of proximate and ultimate analysis [23, 24].

$$N_{CT} = \frac{Y_{C,ult}^2}{Y_{H,ult} \cdot Y_{O,ult}} \tag{2a}$$

$$Y'_{VM} = exp\left[0.031 - 0.029 ln N_{CT} - 0.038\left(ln N_{CT}\right)^2\right] \tag{2b}$$

$$f_5(T) = 3.87\left(\frac{T}{900}\right)^5 - 28.28\left(\frac{T}{900}\right)^4 \\ + 80.87\left(\frac{T}{900}\right)^3 - 112.8\left(\frac{T}{900}\right)^2 \\ + 77.07\left(\frac{T}{900}\right) - 20.26 \tag{2c}$$

$$Y'_{VY} = Y'_{VM} \cdot exp\left[f_5(T)\right] \tag{2d}$$

$$V_E = \frac{Y'_{VY}}{Y'_{VM}} = \frac{Y_{VY}}{Y_{VM}} \qquad (2e)$$

$$Y_{char} = 1 - Y_{VY} = 1 - \sum Y_i \qquad (3a)$$

$$Y_{C,ult} = Y_{char} + \sum \left(\frac{Y_{C,i}.Ar_C}{Mr_i} \right) \qquad (3b)$$

$$Y_{H,ult} = \sum \left(\frac{Y_{H,i}.Ar_H}{Mr_i} \right) \qquad (3c)$$

$$Y_{O,ult} = \sum \left(\frac{Y_{O,i}.Ar_O}{Mr_i} \right) \qquad (3d)$$

$$Y_{N,ult} = \sum \left(\frac{Y_{N,i}.Ar_N}{Mr_i} \right) \qquad (3e)$$

where Y_{VY} is the actual devolatilized products mass fraction, Y_{VM} is the volatile matter mass fraction from proximate analysis on dry-ash-free basis, Y_i is the ith component of actual devolatilized products mass fraction, Y_{char} is the char fraction, $Y_{C,i}$ is the number of C atoms in ith component, $Y_{H,i}$ is the number of H atoms in ith component, $Y_{O,i}$ is the number of O atoms in ith component, $Y_{N,i}$ is the number of N atoms in i^{th} component, Y_{ult} is the C–H–O–N content ultimate analysis in dry-ash-free basis, Ar is the atomic weight for C–H–O–N, and Mr_i is the molecular weight of ith component.

In the rice husk combustor, all devolatilized products will react with oxygen from the air. The air amount was varied under stoichiometric and excess conditions. The excess air (EA) is calculated from Eq. 4 and the O_2 and CO_2 percentages in the flue gas are acquired from Eq. 5, respectively. The exit flue gas temperature was also varied from 200 to 700 °C. All the inputted data for calculation are summarized in Table 2.

Table 2 Inputted data for realistic decomposition calculation

Parameters	Values
Temperature at proximate analysis	900 °C
Decomposition and combustion temperature	700 °C
Excess air	0%, 10%, 20%, 40%, 80%, 100%, 150%, and 200%
Exit flue gas temperature	200 °C, 300 °C, 400 °C, 500 °C, 600 °C, and 700 °C

$$EA = \frac{n_a - n_s}{n_s} \times 100\% \qquad (4)$$

$$O_2\ in\ flue\ gas = \frac{n_{O_2,a} - n_{O_2,s}}{n_{fg}} \times 100\% \qquad (5a)$$

$$CO_2\ in\ flue\ gas = \frac{n_{CO_2}}{n_{fg}} \times 100\% \qquad (5b)$$

where n_a is the actual air amount; n_s is the stoichiometric air amount; $n_{O_2,a}$ is the actual oxygen amount; $n_{O_2,s}$ is the stoichiometric oxygen amount; and n_{CO_2} is the carbon dioxide amount; and n_{fg} is the flue gas amount.

Combustion Efficiency and Adiabatic Flame Temperature (AFT) Calculation

Combustion efficiency and AFT determinations require inlet and outlet enthalpy calculations. The enthalpy calculation considered residual enthalpy (H^R) from Pitzer-Lee-Kesler generalized correlation which involves acentric factor (ω) and critical temperature (T_c) properties [30]. Inlet enthalpy (H_{in}) was derived from biomass and air inlet enthalpy, following Eq. 6. Outlet enthalpy (H_{out}) calculation was given in Eq. 7 which considered ash and flue gas sensible heat. Heat loss (H_{loss}) due to radiation occupied as much as 5% from inlet enthalpy. This percentage of heat loss due to radiation is chosen following the rule of thumb for combustion efficiency improvement in industrial boilers and furnaces [31]. The heat capacity for each component (Cp_i) was a temperature-dependent polynomial function and the reference temperature (T_{ref}) was set at 25 °C. All properties constant were adapted from common databanks [30, 32, 33].

Combustion efficiency (η_c) is derived from the difference between inlet and outlet enthalpy including heat loss, Eq. 8 [8, 31]. Apart from that, the AFT calculation on various excess air was performed with two types of assumption, i.e. no heat loss (perfect insulation) and 5% heat loss due to radiation. The AFT with no heat loss was iteratively calculated by finding T_{out} until inlet enthalpy (Eq. 6) is equal to outlet enthalpy (Eq. 7). AFT calculation with 5% heat loss is to find T_{out} until Eq. 6 has the same value as Eq. 7 and heat loss amount.

$$H_{in} = \left(m_{biomass}.HV_{biomass} \right) + m_{in,i} \cdot \left[\left\{ \sum_{i=1}^{n} \int_{T_{ref}}^{T_{in}} Cp_i\, dT \right\} + H_{in}^R \right] \qquad (6)$$

$$H_{out} = \left(m_{ash} \cdot \int_{T_{ref}}^{T_{out}} Cp_{ash} \cdot dT \right)$$
$$+ m_{out,i} \cdot \left[\left\{ \sum_{i=1}^{n} \int_{T_{ref}}^{T_{out}} Cp_i \cdot dT \right\} + H_{out}^R \right] \quad (7)$$

$$\eta_c = \left(1 - \frac{H_{out} + H_{loss}}{H_{in}} \right) \times 100\% \quad (8)$$

where $m_{biomass}$ is the mass of biomass, $HV_{biomass}$ is biomass calorific value, $m_{in,i}$ is the inlet mass of ith component, T_{in} is air inlet temperature, dT is temperature difference, m_{ash} is the mass of ash, T_{out} is gas outlet temperature or exit flue gas temperature, n is the number of components.

Thermodynamics Calculation Procedure

The calculated flue gas composition from biomass oxidation was then corrected due to the Boudouard reaction and homogeneous water gas shift reaction (WGSR). The interaction between flue gas with remaining biomass through Boudouard reaction and WGSR were assumed ideal and the thermodynamics calculation was carried out using the Gibbs energy minimization as seen in Eq. 9 which considers the temperature-dependent of equilibrium constant (K) and the stoichiometric coefficient of each component (v_i) [30]. The iterative calculation should be addressed until the error tolerance is below 10^{-6}.

$$\prod_{i=1}^{n} (y_i \phi_i)^{v_i} = K \quad (9)$$

The calculation entangled fugacity coefficient (ϕ) and was determined using a generic cubic equation of state, as served in Eq. 10. The equation involved the compressibility factor (Z) which was calculated using Redlich-Kwong, Soave–Redlich–Kwong, and Peng-Robinson models [30]. The coefficients of β, q, I, Ω, Ψ, α, σ, and ε for Z calculation were taken from state parameters assignment [30, 34].

$$\phi = exp(Z - 1 - ln(Z - \beta) - qI) \quad (10)$$

Result and Discussion

Problem Preliminary Analysis: Degree of Freedom (DoF)

In this study, rice husk combustion is assumed to occur at 1 bar and feed inlet is assumed at 25 °C. Also, the combustion is considered to be complete, that is when the product has no unburnt carbon content but only rice husk ash [10].
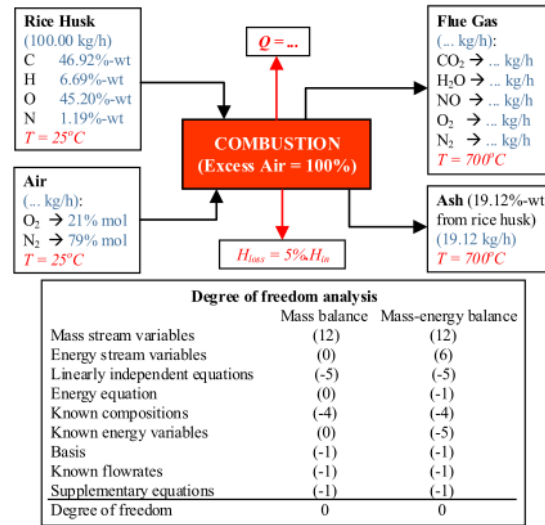

Fig. 1 Rice husk combustion block diagram with DoF analysis

The flue gas produced from the combustion, hence, is composed of CO_2, H_2O, NO, N_2, and the remaining O_2 [17]. NO compound, as one of the NO_X constituents, is chosen due to the process condition tends to form NO than NO_2 or N_2O [4, 5]. The preliminary analysis in the form of DoF is conducted to determine the problem completion criteria. DoF is important and extensively used to give a good indication of whether the material energy balance problem is able to be solved or not [25]. Figure 1 served the rice husk combustion block diagram embedded with DoF analysis.

In accordance with the DoF calculation, there are 6 inlet stream variables (C, H, O, N, O_2, and N_2) and 6 outlet stream variables (CO_2, H_2O, NO, O_2, N_2, and ash). This problem has 1 basis (100 kg/h rice husk) and the number of linearly independent equations is 5 (C, H, O, N, and ash). The known compositions are 4 (C, H, O, and O_2) while the known flowrate is only 1 (ash flowrate). There is also 1 supplementary equation used in this study, i.e. excess air 100%, which is utilized for determining air flowrate amount. On the other hand, the energy stream variables appear as much as 6 (temperature in rice husk stream, temperature in air stream, temperature in flue gas stream, temperature in ash stream, heat loss, and heat released). The known energy variables are 5, composed of 4 known temperatures and 1 known value of heat loss. It can be seen that DoF value is equal to 0 for both mass balance and mass-energy balance, which implies the problems are well-specified and able to be solved either separately (decoupled) or simultaneously (coupled) [25].

Calculation Result Using Realistic Decomposition

The calculation for air inlet condition should utilize the real (non-ideal) gas approach and for the exit flue gas condition is permitted to fulfill the ideal gas approach. Flue gas pressure and temperature conditions neglect the intermolecular interactions due to the high kinetic energy, which reflects the ideal gas characteristics [35]. When the temperature becomes lower to resemble the inlet condition, kinetic energy becomes low and allows for significant intermolecular interactions [32, 34, 35]. Consequently, a real gas approach for inlet state should be considered. Despite the method developed by Thunman et al. can calculate the decomposed products amount, the element balances were only validated with ultimate analysis [26]. In contrast, this study pronounces the necessity to meet mass balance with ultimate and proximate analysis. This concept becomes a novel finding for predicting the actual decomposed products.

According to the realistic decomposition approach calculation, the N_{CT} for rice husk is 7.3 and the decomposition at 700 °C (V_E value = 0.91) leads to the production of 64.78% gas, 7.28% liquid/tar, and 27.94% solid/char, as schemed in Fig. 2. Since the decomposition occurs at 700 °C, the volatile gas and liquid product are mostly obtained and result in less amount of char [28]. Furthermore, the secondary cracking of the liquid product also contributes to tar composition weakening and enriches gas composition, as a consequence [36]. To reinforce the statement, the research on fast pyrolysis of cellulose and wood along with higher temperature from 400 to 800 °C by Scott et al. declared that gas yield increased approximately from 5 to 60%, solid yield lessened approximately from 28 to 2%, and liquid yield increased initially from 70 to 82% but further diminished to about 38% [37].

The gas product is dominated by H_2O (34.62%), CO_2 (30.03%), and CO (26.69%) while minor compounds are found in the form of H_2 (4.76%), NH_3 (2.12%), and CH_4

(1.78%). Methane has the lowest composition and this value is still within the typical composition range of agricultural residue pyrolysis at 400–700 °C, 0.2–2.2% [36, 38]. The volatiles gas yielded from wood thermal decomposition through heat and mass balances modelling conducted by Thunman et al. approximately consists of 18–21% H_2O, 20–25% CO, 18–22% CO_2, 6–12% H_2, and the rest is light hydrocarbon [26]. The difference of temperature (850 °C from their study vs. 700 °C in this study) as well as dissimilar assumptions of volatile gas constituents provokes a slight discrepancy in results. Hernowo has compared the gas yield from prediction using a realistic decomposition approach and from other researchers' experiments for several types of biomass, i.e. corncob (N_{CT} = 15.2), beech wood (N_{CT} = 8.6), and rice straw (N_{CT} = 6.5). Interestingly, the predicted gas yields were closely fit to the experimental results [39, 40] thus ensuring a realistic decomposition approach has well performance in predicting the decomposed products composition.

The gas product also contains NH_3 (2.12%) which is generated from the partial oxidation of N-content in biomass under low-temperature combustion [41]. The NH_3 composition in this study is much lower than from wood bark pyrolysis which was recorded in the range of 4.5–5.5% as well as from bagasse pyrolysis (about 12%) [27]. Other than that, the major components of liquid products are 2-methoxy-5-propyl-phenol and followed by cresol. Quinoline has a composition of 7.13% which is close to typical heterocyclic compounds composition in tar, 6.5% [28]. Hereafter, the liquid product composition result is still plausible since tar is majorly occupied by one-ring aromatic hydrocarbons such as benzene and phenol derivates [28, 29].

The rate of biomass oxidation is much slower than decomposition (to produce gas, liquid, and solid), so providing excess air in the combustion stage must be applied, as a consequence [28]. This study used 100% excess air which is still in the range of common excess air amount
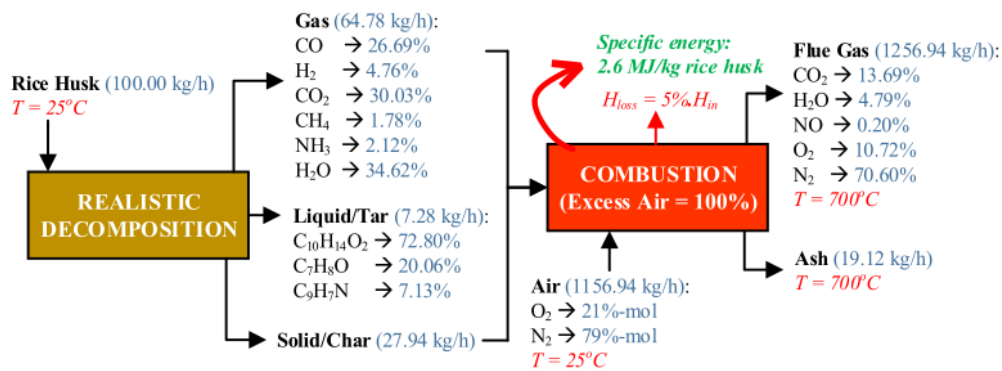

Fig. 2 Rice husk combustion calculation based on realistic decomposition approach

for rice husk combustion, 40–100% [42]. The calculated air amount is 1156.94 kg/h and as much as 1276.06 kg/h of flue gas is generated with the composition of 13.69% CO_2, 4.79% H_2O, 0.19% NO, 70.60% N_2, and 10.72% remaining O_2. Likewise, about 2.6 MJ/kg specific combustion energy from rice husk is released at exit flue gas temperature of 700 °C with 5% heat loss. The value is still in the range as stated by Chang et al. (2.12–3.00 MJ/kg) [14] and also quite similar to the research conducted by Memon et al. (2.77 MJ/kg) [15]. Interestingly, Kwofie et al. observed that 7.53 MJ/kg of specific combustion energy from rice husk was able to be generated due to the direct application of cogeneration by means of steam generator and hot air generator [16]. All of the results imply the calculation using a realistic decomposition approach has reasonable and logical performance when compared to the several rice husk combustion experiments from other researchers.

The mass and energy balances calculation is further able to deliver a nomogram to interpret the relation between O_2 or CO_2 concentration in the flue gas and excess air used in the combustion process [16]. Usually, the combustor is equipped with O_2 or CO_2 detector which is installed at the outlet pipe to record the concentration. In absence of gas detector, the flue gas could also be analyzed through gas chromatography to ensure the O_2 and CO_2 amount [43]. The

rice husk combustion nomogram in Fig. 3 has a similar pattern with the combustion efficiency charts for natural gas, No. 2 fuel oil, and No. 6 fuel oil [44]. Nomogram in Fig. 3 exhibits that combustion efficiency alleviation under higher flue gas temperature is somewhat significant rather than under large excess air supply. Combustion efficiency represents the effective heat utilized in the combustion process where its value is lower at a higher excess air and flue gas temperature [7, 8, 31]. The red line describes that about 10% of O_2 or 9% of CO_2 in the flue gas will be detected if 50% of excess air is involved in the combustion. In this condition, the combustion efficiency is about 77% at flue gas temperature of 200 °C and declining to 21% at 700 °C. When flue gas contains higher oxygen content (blue line), 18% of O_2 or 8.2% of CO_2, it means that the combustion takes place using 100% of excess air. At this condition, the combustion efficiency is 74% at flue gas temperature of 200 °C and reduce to 15% at 700 °C.

To convince the results, the combustion efficiency using natural gas, No. 2 fuel oil, and No. 6 fuel oil at flue gas temperature of 200 °C and excess air of 100% were 83%, 86%, and 87%, in a successive term [44]. It is realized that No. 6 fuel oil has the highest calorific value and then followed by No. 2 fuel oil, natural gas, and rice husk, with declining values [45]. This is the cause for the lowest combustion efficiency of rice husk when compared to the three fossil fuels aforementioned. In addition, as much as 21% of combustion energy loss is dominated by the high flue gas sensible heat (known as flue gas loss) and 5% due to radiation since this calculation ignores the incomplete combustion loss and unburnt carbon loss. This argument is strengthened by the study of heat balance for boiler efficiencies calculation carried out by Patro where energy loss at flue gas temperature of 180–183 °C occupies as much as 28.88–25.98% [46].

At higher excess air, nitrogen as an inert gas absorbs the heat from combustion and carries it out from the combustor [47]. This impacts on reducing combustion effective heat and lead to low combustion efficiency. The higher flue gas temperature at a constant excess air amount will also lead to poorer combustion efficiency because high flue gas temperature indicates the heat has already flown out from the combustor before it is used for combustion purposes. Accordingly, it is important to utilize the flue gas sensible heat through cogeneration or combine cycle to enhance the combustion efficiency [14, 48, 49], as proven by Kwofie et al. [16]. Yet, the minimum allowable exit flue gas temperature is usually at 200 °C to prevent flue gas condensation [50]. This exit flue gas temperature also complies with the rule of thumb which normally ranges from 175 to 260 °C [31].
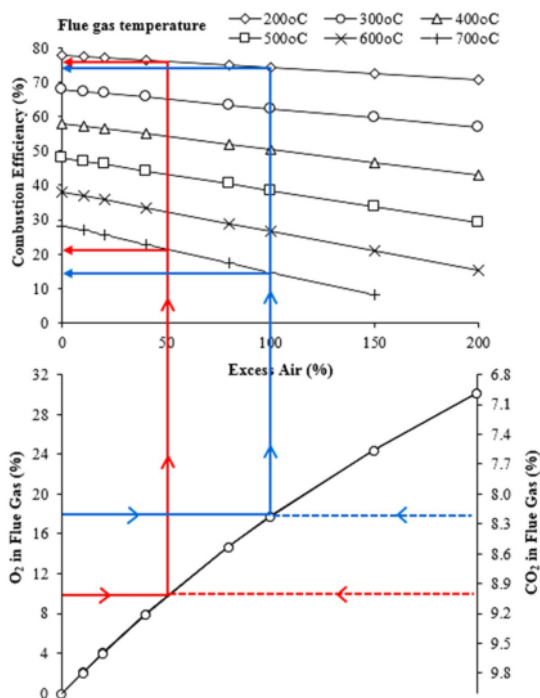

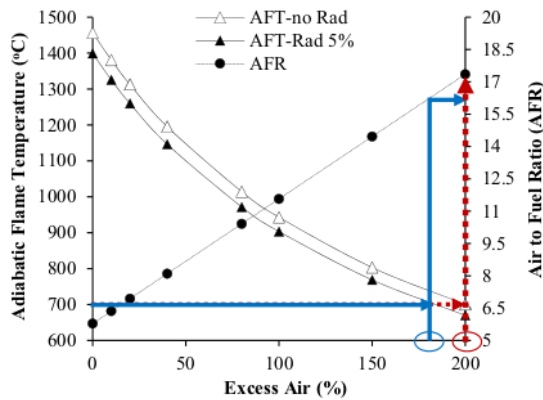**Fig. 3** Rice husk combustion efficiency nomogram

Fig. 4 AFT for rice husk combustion at various excess air

Adiabatic Flame Temperature (AFT) and Air Supply Strategy for Rice Husk Combustion

AFT is the highest theoretical temperature achieved at perfect insulation of the combustion process which is unique for each fuel and only depends on calorific value as long as in absence of molecules dissociation [51]. The maximum value of AFT is reached when the stoichiometric air is supplied [52]. Based on the calculation, rice husk combustion has a maximum temperature of up to 1457 °C under perfect insulation. This value is slightly higher than the highest temperature of rice husk combustion under stoichiometric condition from Anshar et al. which was 1407 °C. This is due to the lower calorific value of biomass in their study, 13.44 MJ/kg [17].

Subsequently, this study expresses that heat loss due to radiation gives a quite lower AFT with a discrepancy around 30–60 °C as notified in Fig. 4. Up to now, there is still a lack of studies that directly observe the effect of heat loss due to radiation on decreasing AFT. However, a study carried out by Li et al. could give a comparison since the combusted biomass was wood with a calorific value that is quite close to rice husk, which is 13.36 MJ/kg. They measured the heat loss due to a 5% moisture increase in wood combustion lowering the AFT by a value of 40–70 °C [53]. Again, the realistic decomposition approach shows its ability to predict the highest rice husk combustion temperature with a rational result with other studies.

Similar to the previous explanation that larger excess air promotes more significant convective heat flow and impacts on reducing AFT [53], Fig. 4. It turns out that nitrogen in excess air also dilutes and cools down the flue gas temperature due to the sensible heat absorption [47]. The identical pattern is found that AFT from wood combustion changed from 1377 to 1307 °C under higher excess air from 21 to

33% [53]. This figure also announces that under 100% excess air, the adiabatic flame temperature for rice husk combustion is 903–943 °C. If rice husk combustion temperature exceeds 700 °C, the silica in ash tends to be crystalline which could threaten human respiratory systems [5, 54]. Hence, it is important to maintain the rice husk combustion temperature at 700 °C by supplying 200% excess air or air to fuel ratio (AFR) of 17.35 in the combustor under perfect insulation. If there is a 5% heat loss due to radiation, the excess air supply of about 180% or AFR 16.19 is still allowable.

Flue Gas Composition Analysis

The biomass thermal process through combustion is a complex set of reactions that produces CO, H_2, CO_2, H_2O, NO, N_2, and remaining O_2 [6, 13]. The calculated fugacity coefficient is 1 for ideal gas and between 0–1 for real gas, which means that there is an intermolecular force attraction [35]. Nevertheless, there is a condition that the fugacity coefficient value is more than 1 which informs that there is an intermolecular force repulsion [34, 35]. The fugacity coefficient for all related gas is depicted in Fig. 5 and calculation with Redlich-Kwong, Soave–Redlich–Kwong, and Peng-Robinson models show slightly similar results. It is also shown that the gas acts more ideal at a higher temperature, which is characterized by the average fugacity coefficient that is closer to 1 [30, 34]. The fugacity coefficient value is then used for Gibbs Energy minimization calculation to predict the flue gas composition.

At a temperature of up to 700 °C, the complete oxidation of compounds based on C and H atoms are still spontaneous whereas an opposite pattern is found for N atom [7, 30]. When returning to the mass and energy balances calculation
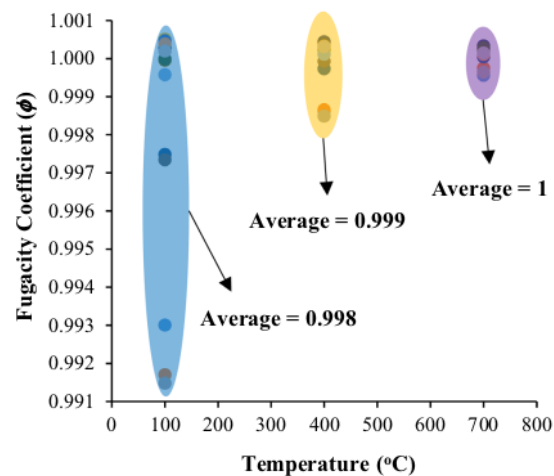

Fig. 5 Flue gas fugacity coefficient at various temperatures

in Fig. 2, it is exhibited that NO in the flue gas occupies as much as 0.20% or 25.4 g NO is generated from 1 kg of combusted rice husk. Meanwhile, thermodynamics calculation reveals that NO (on behalf of the major NO_X compound) has a very low equilibrium constant, 3.88×10^{-4} at 700 °C [4]. Moreover, biomass combustion is frequently undergone at below 1000 °C because it uses a large amount of excess air as well as biomass inferior calorific value compared to fossil fuel, which leads to the negligence of the NO_X emission value [4, 5, 7, 41].

On the other hand, CO_2 and H_2O are spontaneously formed and the CO produced from the decomposition will immediately convert to CO_2 when air is supplied surpassing its stoichiometric value. Under excess air conditions, the reaction between excess O_2 and CO to form CO_2 is more spontaneous rather than the reaction with H_2 to form H_2O (Gibbs free energy change comparison: $-257,190$ kJ/mol vs. $-228,572$ kJ/mol) [30, 33]. Also, Simonov et al. affirmed that CO reaction with O_2 could swiftly undergo to form CO_2 [55]. Nonetheless, the further reaction between unburnt biomass and CO_2 in the combustor to form CO again through Boudouard reaction could occur. Hereafter,

the CO produced from Boudouard reaction has a chance to react with H_2O to form H_2 through homogeneous WGSR [55, 56]. This is suspected to be the cause of the CO and H_2 formation even though the combustion is held using excess air and takes place at a temperature of more than 700 °C.

In pursuance of the single reaction simulation, the Boudouard reaction is feasible only when the temperature surpasses 500 °C [55]. The equilibrium conversion of this reaction is higher along with the increasing temperature, due to the endothermic reaction. The opposite pattern is applied for homogeneous WGSR, an exothermic reaction that could spontaneously undergo at a lower temperature but the equilibrium conversion decreases at a larger temperature [57]. For simultaneous reaction, WGSR occurs only when the temperature is above 500 °C due to the CO compound being produced above this temperature. The equilibrium conversion for both single reactions is shown in Fig. 6a and the conversion of the simultaneous reaction is plotted in Fig. 6b.

The mass and energy balances calculation could determine the flue gas composition of a completed oxidation reaction (Fig. 2), but the composition should be corrected due to the presence of simultaneous reaction of Boudouard-WGSR

Fig. 6 Equilibrium conversion for Boudouard and WGSR: single reaction (**a**) and simultaneous reaction (**b**)
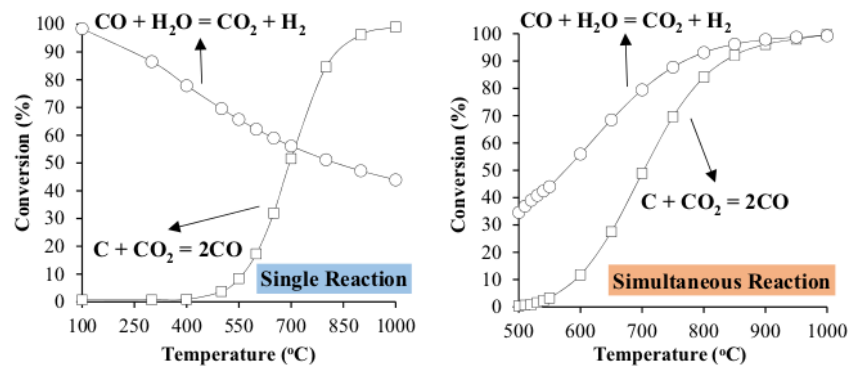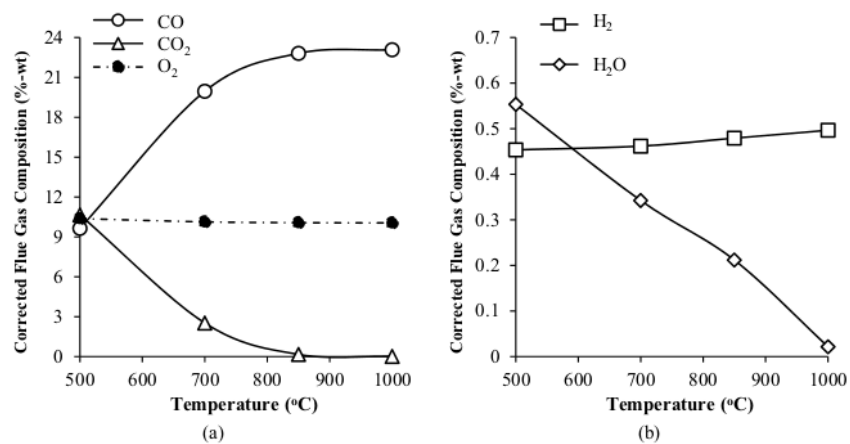

Fig. 7 Corrected flue gas composition after considering the simultaneous reaction of Boudouard-WGSR

[28, 55, 56]. The corrected flue gas composition at various temperatures can be seen in Fig. 7. The figure informs that CO composition changes from 9.65 to 23.08% as well as CO_2 composition diminishes from 10.65 to 0.02% as the temperature rises from 500 to 1000 °C. Besides that, H_2 composition also intensifies from 0.45 to 0.50% as well as H_2O composition alleviates from 0.55 to 0.02% in line with higher temperature. The CO and H_2 amount enrichment are also discovered in the thermodynamics analysis of biomass thermal decomposition conducted by Li et al., where at the operating temperature of 700–850 °C, CO yield was obtained higher from 0.56 to 0.66 Nm^3/kg, H_2 yield was upgraded from 0.10 to 0.25 Nm^3/kg, and CO_2 yield was decreasing from 0.30 to 0.25 Nm^3/kg [58]. Likewise, the CO and H_2 composition from wood thermal decomposition were also intensified along with temperature change from 400 to 600 °C [59].

The corrected flue gas amount at 700 °C from thermodynamics calculation now has a composition of 2.52% CO_2,

0.34% H_2O, 19.95% CO, 0.46% H_2, 66.70% N_2, and 10.13% remaining O_2. The CO, which was produced from the simultaneous reaction of Boudouard-WGSR at above 500 °C, is imperative to reduce the amount for it is toxic to humans. Following Le-Chatelier principles, providing excess air could allow the CO spontaneous reaction with oxygen to form CO_2 [56, 60]. Thus, maintaining rice husk combustion temperature at 700 °C, aside from preventing NO_X formation and avoiding the silica in ash phase transformation into crystalline, can also suppress the CO amount [5, 7, 12, 54, 61]. As a final summary, the calculation results from the realistic decomposition approach in this study compared to other studies are outlined in Table 3.

Table 3 The results comparison between realistic decomposition approach (this study) and other studies

Variables	Results from this study	Results from other studies
Biomass decomposition products	Rice husk, T = 700 °C Gas: 64.78% Liquid/tar: 7.28% Solid/char: 27.94%	Wood, T = 800 °C Gas: 60% Liquid/tar: 38% Solid/char: 2% Ref.: [37]
H_2O, CO_2, CO, and H_2 composition in gas product	Rice husk, T = 700 °C 34.62%, 30.03%, 26.69%, 4.76%	Wood, T = 850 °C 18–21%, 18–22%, 20–25%, 6–12% Ref.: [26]
NH_3 composition in gas product	Rice husk: 2.12%	Wood bark: 4.5–5.5% Bagasse: About 12% Ref.: [27]
CH_4 composition in gas product	Rice husk: 1.78%	Agricultural residue: 2.2% Ref.: [36, 38]
Quinoline composition in liquid/tar product	7.13%	6.5% Ref.: [28]
Rice husk specific combustion energy	2.6 MJ/kg	2.12–3.00 MJ/kg Ref.: [14] 2.77 MJ/kg Ref.: [15] 7.53 MJ/kg Ref.: [16]
Combustion efficiency at 100% of excess air and 200 °C of exit flue gas temperature	Rice husk: 79% (only flue gas loss)	Natural gas: 83% No. 2 fuel oil: 86% No. 6 fuel oil: 87% Ref.: [44, 45]
Flue gas loss	Rice husk combustor: 21% Flue gas temperature: 200 °C	Boiler: 28.88–25.98% Flue gas temperature: 180–183 °C Ref.: [46]
Maximum value of adiabatic flame temperature (AFT) for rice husk combustion	1457 °C	1407 °C Ref.: [17]
AFT profile under higher excess air amount	Rice husk: Declining from 1313 °C to 1195 °C (excess air from 20 to 40%)	Wood: Declining from 1377 °C to 1307 °C (excess air from 21 to 33%) Ref.: [53]
The magnitude of AFT decrease	Rice husk: 30–60° under heat loss due to radiation of 5%	Wood: 40–70° under heat loss due to moisture increase of 5% Ref.: [53]

Conclusion and Suggestion

The thermodynamics simulation performance of rice husk combustion with a realistic decomposition approach on the devolatilization stage has been studied. From this study, the results from this approach give a close comparison with the other researchers' results in terms of the amount and composition of devolatilized products, the amount of specific combustion energy, adiabatic flame temperature, and flue gas composition. Under calculation with the realistic decomposition approach, rice husk devolatization produce 64.78% gas, 7.28% liquid/tar, and 27.94% solid/char which are then oxidized by 100% excess air to produce flue gas with the composition of 13.69% CO_2, 4.71% H_2O, 0.20% NO, 70.60% N_2, and 10.72% remaining O_2. About 2.6 MJ/kg specific combustion energy from rice husk is also released at a flue gas temperature of 700 °C with 5% heat loss. From this study, rice husk with 14.95 MJ/kg of calorific value could achieve the highest theoretical combustion temperature around 1457 °C for perfect insulation while under 5% heat loss due to radiation could reduce the combustion temperature by about 30–60 °C. According to the thermodynamics simulation, NO_X emission is extremely low as long as the combustion temperature is still below 700 °C. Also, the CO and H_2 emissions are still possible to exist even combustion take place at more than 700 °C with 100% excess air as long as CO_2 reacts with the remaining biomass through the simultaneous reaction of Boudouard-WGSR. The corrected flue gas amount at 700 °C from thermodynamics calculation now has a composition of 2.52% CO_2, 0.34% H_2O, 19.95% CO, 0.46% H_2, 66.70% N_2, and 10.13% remaining O_2. Although biomass combustion temperature is definitely lower than fossil fuel combustion, maintaining rice husk combustion below 700 °C is a necessity to reduce NO_X and CO emissions as well as preventing silica in ash phase change to crystalline which harms humans. Providing excess air of about 180–200% could be an alternative solution for the problems.

Declarations

Conflict of interest There is no conflict or competing of interest to declare.

References

1. Budhi, Y.W., Effendy, M., Bindar, Y., Subagjo, S.: Dynamic behavior of reverse flow reactor for lean methane combustion. J. Eng. Technol. Sci. **46**, 299–317 (2014)
2. Karim, M.R., Ovi, I.R.Q., Naser, J.: A CFD model for biomass combustion in a packed bed furnace. AIP Conf. Proc. (2016). https://doi.org/10.1063/1.4958417
3. Panuju, D.R., Mizuno, K., Trisasongko, B.H.: The dynamics of rice production in Indonesia 1961–2009. J. Saudi Soc. Agric. Sci. **12**, 27–37 (2013). https://doi.org/10.1016/j.jssas.2012.05.002
4. Steven, S., Ramli, Y., Pratama, D., Restiawaty, E., Bindar, Y.: Life cycle analysis (LCA) for silica production from three different routes: Conventional, fume, and green routes. In: International Seminar on Chemical Engineering Soehadi Reksowardojo (STKSR) in conjunction with Symposium on Photocatalyst and Photocatalysis. p. 111 (2020)
5. Steven, S., Restiawaty, E., Bindar, Y.: Routes for energy and bio-silica production from rice husk: a comprehensive review and emerging prospect. Renew. Sustain. Energy Rev. **149**, 111329 (2021). https://doi.org/10.1016/j.rser.2021.111329
6. Demirbas, A.: Combustion characteristics of different biomass fuels. Prog. Energy Combust. Sci. **30**, 219–230 (2004). https://doi.org/10.1016/j.pecs.2003.10.004
7. Werther, J., Saenger, M., Hartge, E.U., Ogada, T., Siagi, Z.: Combustion of agricultural residues. Prog. Energy Combust. Sci. **26**, 1–27 (2000). https://doi.org/10.1016/S0360-1285(99)00005-2
8. Armesto, L., Bahillo, A., Veijonen, K., Cabanillas, A., Otero, J.: Combustion behaviour of rice husk in a bubbling fluidised bed. Biomass Bioenerg. **23**, 171–179 (2002). https://doi.org/10.1016/S0961-9534(02)00046-6
9. Steven, S., Restiawaty, E., Pasymi, P., Bindar, Y.: An appropriate acid leaching sequence in rice husk ash extraction to enhance the produced green silica quality for sustainable industrial silica gel purpose. J. Taiwan Inst. Chem. Eng. **122**, 51–57 (2021). https://doi.org/10.1016/j.jtice.2021.04.053
10. Steven, S., Restiawaty, E., Pasymi, P., Bindar, Y.: Influences of pretreatment, extraction variables, and post-treatment on bench-scale rice husk black ash (RHBA) processing to bio-silica. Asia-Pac. J. Chem. Eng. **16**, e2694 (2021). https://doi.org/10.1002/apj.2694
11. Steven, S., Restiawaty, E., Bindar, Y.: Simple mass transfer simulation using a single-particle heterogeneous reaction approach in rice husk combustion and rice husk ash extraction. In: International Bioprocessing Association Subject Conference (IBASC) on Sustainable Technologies for Bioresource Utilization: Bio-based Products, Bioenergy, and Environmental Protection. p. 128 (2021)
12. Vassilev, S.V., Baxter, D., Vassileva, C.G.: An overview of the behaviour of biomass during combustion: Part I. Phase-mineral transformations of organic and inorganic matter. Fuel **112**, 391–449 (2013). https://doi.org/10.1016/j.fuel.2013.05.043
13. Nunes, L.J.R., Matias, J.C.O., Catalão, J.P.S.: Mixed biomass pellets for thermal energy production: a review of combustion models. Appl. Energy. **127**, 135–140 (2014). https://doi.org/10.1016/j.apenergy.2014.04.042
14. Chang, C.T., Costa, M., Villetta, M. La: Thermodynamic and economic analysis of a combined CHP system fuelled with rice husk. (2017)
15. Memon, T.A., Harijan, K., Soomro, M.I., Meghwar, S., Valasai, G.D., Khoharo, H.: Potential of electricity generation from rice husk: A case study of rice mill. Sindh Univ. Res. J. Sci. Ser. **49**, 495–498 (2017). https://doi.org/10.26692/surj/2017.09.05
16. Kwofie, E.M., Ngadi, M., Sotocinal, S.: Thermodynamic evaluation of a rice husk fired integrated steam and hot air generation

unit for rice parboiling. Energy **128**, 39–49 (2017). https://doi.org/10.1016/j.energy.2017.04.013

17. Anshar, M., Ani, F.N., Kader, A.S.: Combustion characteristics modeling of rice husk as fuel for power plant in Indonesia. Appl. Mech. Mater. **695**, 815–819 (2014). https://doi.org/10.4028/www.scientific.net/amm.695.815

18. Karim, M.R., Naser, J.: CFD modelling of combustion and associated emission of wet woody biomass in a 4 MW moving grate boiler. Fuel **222**, 656–674 (2018). https://doi.org/10.1016/j.fuel.2018.02.195

19. Gómez, M.A., Porteiro, J., Patiño, D., Míguez, J.L.: CFD modelling of thermal conversion and packed bed compaction in biomass combustion. Fuel **117**, 716–732 (2014). https://doi.org/10.1016/j.fuel.2013.08.078

20. Karim, M.R., Bhuiyan, A.A., Sarhan, A.A.R., Naser, J.: CFD simulation of biomass thermal conversion under air/oxy-fuel conditions in a reciprocating grate boiler. Renew. Energy. **146**, 1416–1428 (2020). https://doi.org/10.1016/j.renene.2019.07.068

21. ANSYS: ANSYS Fluent Theory Guide 2019 R3. (2019)

22. Bindar, Y.: Computational engineering on multidimensional turbulent flows (Rekayasa Komputasi Aliran Turbulen Multidimensi). (2017)

23. Bindar, Y., Riza, A., Susanto, H., Sasongko, D.: Coal decomposition method based on element balance and devolatilization theory from proximate and ultimate analysis data. J. Tek. Kim. Indones. **6**, 549–562 (2007)

24. Bindar, Y.: New correlations for coal and biomass pyrolysis performances with coal-biomass type number and temperature. J. Eng. Technol. Sci. **45**, 275–293 (2013)

25. Reklaitis, G. V.: Introduction to Material and Energy Balances. (1983)

26. Thunman, H., Niklasson, F., Johnsson, F., Leckner, B.: Composition of volatile gases and thermochemical properties of wood for modeling of fixed or fluidized beds. Energy Fuels **15**, 1488–1497 (2001). https://doi.org/10.1021/ef010097q

27. Hansson, K.-M., Samuelsson, J., Tullin, C., Åmand, L.-E.: Formation of HNCO, HCN, and NH3 from the pyrolysis of bark and nitrogen-containing model compounds. Combust. Flame. **137**, 265–277 (2004). https://doi.org/10.1016/j.combustflame.2004.01.005

28. Basu, P.: Biomass Gasification, pyrolysis and torrefaction: practical design and theory. (2013)

29. Saad, A., Ratanawilai, S., Tongurai, C.: Catalytic conversion of pyrolysis tar to produce green gasoline-range aromatics. Energy Procedia. **79**, 471–479 (2015). https://doi.org/10.1016/j.egypro.2015.11.521

30. Smith, J.M., Van Ness, H.C., Abbott, M.M.: Introduction to chemical engineering thermodynamics, Seventh Edition. (2005)

31. Dockrill, P., Friedrich, F.: Boilers and heaters: improving energy efficiency. Natural Resources Canada (2001)

32. Poling, B.E., Prausnitz, J.M., O'Connell, J.P.: The Properties of Gases and Liquids, Fifth Edition. (2001)

33. Poling, B.E., Thomson, G.H., Friend, D.G., Rowley, R.L., Wilding, W.V.: Physical and chemical data. In: Perry's Chemical Engineers' Handbook, 8th edition. pp. 2–517 (2008)

34. Prausnitz, J.M., Lichtenthaler, R.N., de Azevedo, E.G.: Molecular thermodynamics of fluid-phase equilibria, Third Edition. (1999)

35. Atkins, P., de Paula, J.: Physical chemistry, Ninth Edition. (2010)

36. Nunn, T.R., Howard, J.B., Longwell, J.P., Peters, W.A.: Product compositions and kinetics in the rapid pyrolysis of sweet gum hardwood. Ind. Eng. Chem. Process Des. Dev. **24**, 836–844 (1985). https://doi.org/10.1021/i200030a053

37. Scott, D.S., Piskorz, J., Bergougnou, M.A., Graham, R., Overend, R.P.: The role of temperature in the fast pyrolysis of cellulose and wood. Ind. Eng. Chem. Res. **27**, 8–15 (1988). https://doi.org/10.1021/ie00073a003

38. Di Blasi, C., Signorelli, G., Russo, C.D., Rea, G.: Product distribution from pyrolysis of wood and agricultural residues. Ind. Eng. Chem. Res. **38**, 2216–2224 (1999). https://doi.org/10.1021/ie980711u

39. Hernowo, P., Rasrendra, C.B., Irawan, A., Marno, S., Meliana, Y., Muraza, O., Bindar, Y.: Volatile state mathematical models for predicting components in biomass pyrolysis products. J. Eng. Technol. Sci. **54**, 15878 (2022). https://digilib.itb.ac.id/index.php/gdl/view/57874

40. Hernowo, P., Steven, S., Restiawaty, E., Irawan, A., Rasrendra, C.B., Marno, S., Meliana, Y., Bindar, Y.: Chemicals component yield prediction and kinetic parameters determination of oil palm shell pyrolysis through volatile state approach and experimental study. J. Anal. Appl. Pyrolysis. **161**, 105399 (2022). https://doi.org/10.1016/j.jaap.2021.105399

41. Perez-Jimenez, J.A.: Gaseous emissions from the combustion of biomass pellets. WIT Trans. State Art Sci. Eng. **85**, 87–99 (2015). https://doi.org/10.2495/978-1-84566-062-8/006

42. Singh, R.I., Mohapatra, S.K., Gangacharyulu, D.: Fluidised bed combustion and gasification of rice husk and rice straw—a state of art review. Int. J. Renew. Energy Technol. **2**, 345 (2011). https://doi.org/10.1504/ijret.2011.042727

43. Spindt, R.S.: Air-fuel ratios from exhaust gas analysis. SAE Tech. Pap. Ser. **650507**, 788–793 (1965)

44. Parker, S.A., Walker, B.K.: Boilers and Fired Systems. In: Energy Management Handbook, Eighth Edition. pp. 91–129 (2013)

45. Engineering ToolBox: fuel oil combustion values. (2003)

46. Patro, B.: Efficiency studies of combination tube boilers. Alexandria Eng. J. **55**, 193–202 (2016). https://doi.org/10.1016/j.aej.2015.12.007

47. Rozainee, M., Ngo, S.P., Salema, A.A., Tan, K.G.: Fluidized bed combustion of rice husk to produce amorphous siliceous ash. Energy Sustain. Dev. **12**, 33–42 (2008). https://doi.org/10.1016/S0973-0826(08)60417-2

48. Mehta, D.P.: Waste heat recovery. In: Energy Management Handbook, Eighth Edition. pp. 201–224 (2013)

49. Wong, J.B., Kovacik, J.M.: Cogeneration and distributed generation. In: Energy Management Handbook, Eighth Edition. pp. 161–199 (2013)

50. Shatskikh, Y.V., Sharapov, A.I., Byankin, G.I.: Analysis of deep heat recovery from flue gases. J. Phys. Conf. Ser. **891**, 012188 (2017)

51. Ragland, K.W., Bryden, K.M.: Thermodynamics of combustion. In: Combustion Engineering, Second Edition. pp. 41–90 (2011)

52. Witte, L.C.: Thermal sciences review. In: Energy Management Handbook, Eighth Edition. pp. 749–770 (2013)

53. Li, C., Gillum, C., Toupin, K., Donaldson, B.: Biomass boiler energy conversion system analysis with the aid of exergy-based methods. Energy Convers. Manag. **103**, 665–673 (2015). https://doi.org/10.1016/j.enconman.2015.07.014

54. Dizaji, H.B., Zeng, T., Hartmann, I., Enke, D., Schliermann, T., Lenz, V., Bidabadi, M.: Generation of high quality biogenic silica by combustion of rice husk and rice straw combined with pre- and post-treatment strategies-A review. Appl. Sci. **9**, 1–27 (2019). https://doi.org/10.3390/app9061083

55. Simonov, A.D., Mishenko, T.I.: Combustion and processing of rice husk in the vibrofluidized bed of catalyst or inert material. Chem. Sustain. Dev. **11**, 277–283 (2003)

56. Ganesh, A., Grover, P.D., Lyer, P.V.R.: Combustion and gasification characteristics of rice husk. Fuel **71**, 889–894 (1992). https://doi.org/10.1016/0016-2361(92)90238-J

57. Choi, Y., Stenger, H.: Kinetics of methanol decomposition and water gas shift reaction on a commercial Cu-ZnO/Al2O3 catalyst. Fuel Chem. Div. Prepr. **47**, 723–724 (2002)

58. Li, Z., Xu, H., Yang, W., Xu, M., Zhao, F.: Numerical investigation and thermodynamic analysis of syngas production through

chemical looping gasification using biomass as fuel. Fuel **246**, 466–475 (2019). https://doi.org/10.1016/j.fuel.2019.03.007

59. Nikitin, N.I.: Chemistry of Cellulose and Wood. (1966)

60. Jose, L.S., Bollini, B.L., DaSilva, M.E., Colombaroli, T.S., Tuna, C.E., Araujo, F.H. de M., Vane, L.F., Pedroso, D.T., Tapia, L.C.F.T., Virgoux, R.Z.: Gibbs free energy as a function of temperature of formation reactions. In: Sustainable Hydrogen Production Processes. p. 183 (2017)

61. Steven, S., Restiawaty, E., Bindar, Y.: A simulation study on rice husk to electricity and silica mini-plant: From organic Rankine cycle (ORC) study to its business and investment plan. In: International Bioprocessing Association Subject Conference (IBASC) on Sustainable Technologies for Bioresource Utilization: Bio-based Products, Bioenergy, and Environmental Protection. p. 127 (2021)

Publisher's Note Springer Nature remains neutral with regard to jurisdictional claims in published maps and institutional affiliations.

Authors and Affiliations

Soen Steven[1] · Pandit Hernowo[2] · Elvi Restiawaty[1,3] · Anton Irawan[4] · Carolus Borromeus Rasrendra[1,5] · Abrar Riza[6] · Yazid Bindar[1,7]

1   Department of Chemical Engineering, Faculty of Industrial Technology, Institut Teknologi Bandung, Jl. Ganesha 10, Bandung 40132, Indonesia

2   Department of Chemical Engineering, Institut Sains Dan Teknologi Al-Kamal, Jakarta Barat 11520, Indonesia

3   Research Group on Design and Development of Chemical Engineering Processes, Faculty of Industrial Technology, Institut Teknologi Bandung, Jl. Ganesha 10, Bandung 40132, Indonesia

4   Department of Chemical Engineering, Faculty of Engineering, Universitas Sultan Ageng Tirtayasa, Jl. Jendral Soedirman km 3 Cilegon, Banten 42135, Indonesia

5   Center for Catalysis and Reaction and Engineering, Faculty of Industrial Technology, Institut Teknologi Bandung, Jl. Ganesha 10, Bandung 40132, Indonesia

6   Department of Mechanical Engineering, Faculty of Engineering, Universitas Tarumanagara, Jl. Letjen S. Parman No. 1, Jakarta Barat 11440, Indonesia

7   Research Group on Biomass and Food Processing Technology, Faculty of Industrial Technology, Institut Teknologi Bandung, Jl. Ganesha 10, Bandung 40132, Indonesia

Thermodynamic Simulation 2022